

Outdoor thermal performance of green roofs across multiple time scales: A case study in subtropical China

Xiandi Zheng ^{a,f}, Fanhua Kong ^{a,*}, Haiwei Yin ^b, Ariane Middel ^c, Hongqing Liu ^{a,f}, Ding Wang ^{a,f}, Tao Sun ^d, Itamar Lensky ^e

^a School of Geography and Ocean Science, Nanjing University, Xianlin Ave.163, 210023, Nanjing, China

^b School of Architecture and Urban Planning, Nanjing University, No. 22, Hankou Road, 210093, Nanjing, China

^c School of Arts, Media and Engineering, School of Computing, Informatics, and Decisions Systems Engineering, Arizona State University, Tempe, AZ, United States

^d State Key Laboratory of Urban and Regional Ecology, Research Center for Eco-Environmental Sciences, Chinese Academy of Sciences, Beijing, 100085, China

^e Department of Geography and Environment, Bar-Ilan University, Ramat-Gan, 5290002, Israel

^f International Institute for Earth System Science (ESSI), Nanjing University, Xianlin Ave.163, 210023, Nanjing, China



ARTICLE INFO

Keywords:

Extensive green roof
Outdoor thermal performance
Influencing factors
Multiple time scales
Subtropical monsoon climate

ABSTRACT

In recent years, roof greening technologies have been developed and implemented worldwide, as green roofs are an effective nature-based solution for alleviating outdoor heat and reducing building energy costs. While most observational green roof studies have investigated the cooling effect of model or test plots, few studies have conducted full-scale measurements; however, to guide green roof implementation, the thermal performance of full-scale roofs is crucial. This experimental study explored the ability of extensive green roofs to reduce outdoor temperatures on multiple time scales. The outdoor cooling effect of green roofs and the main factors that drive its performance were analyzed using long-term observational data collected from May 2016 to April 2019 in Nanjing, China. The results suggest that the cooling effect of green roofs exhibits significant diurnal, seasonal, annual, and vertical trends, and that the cooling performance across different time scales corresponds to weather and soil characteristics. The best cooling effect occurred at a height of 60 cm. The green roof displayed a temporary diurnal warming effect but had a good cooling effect on a seasonal time scale, with the largest amount of cooling occurring during the summer (average of 0.28 °C). The findings of this study can support the development, management, and maintenance of green roofs in subtropical areas.

1. Introduction

Rapid urbanization and overdevelopment negatively impact urban ecological systems (Hallegatte & Corfee-Morlot, 2010). Energy shortages and degradation of the urban eco-environment have increasingly raised concerns worldwide (Santamouris, 2015). Population growth in landlocked urban areas inevitably leads to more compact developments, which increases the urban heat island (UHI) effect and puts more thermal stress on urban populations, especially during hot and humid summers (Cartalis, Synodinou, Proedrou, Tsangrassoulis, & Santamouris, 2001; Hoag, 2015; Ng, Chen, Wang, & Yuan, 2012). Green infrastructure can mitigate the adverse effects of urbanization and improve outdoor human thermal comfort by providing important temperature regulating ecosystem services (Hoffman & McDonough, 2005; Kong et al., 2016). However, the lack of available ground space limits

the construction of large-scale green infrastructure such as parks due to dense urban forms and high economic land values (Mathieu, Freeman, & Aryal, 2007). Thus, green roofs (GRs), also called vegetated roofs or living roofs, known as the fifth facade of a building, have frequently been proposed as a way to increase the amount of green space in urban areas (Castleton, Stovin, Beck, & Davison, 2010). GRs are generally classified into two types: intensive and extensive, depending on the thickness of the growth substrate layer and the type of plant species. An intensive green roof (IGR) is usually thicker (150–400 mm) and the plant species require significant maintenance and irrigation. An extensive green roof (EGR) is used mainly to cover large non-walkable roofs, has a low substrate depth (up to 150 mm), and the plant species require little maintenance (Heusinger & Weber, 2017). Since EGRs have much lower maintenance requirements and are less expensive, they are more widely used than IGRs (Heusinger & Weber, 2017).

* Corresponding author.

E-mail address: fanhuakong@163.com (F. Kong).

As a type of artificial ecosystem away from the ground, GRs can provide many ecosystem services, such as reduced urban runoff (Barnhart et al., 2021; Wang, Tian, & Zhao, 2017), noise reduction (Van Renterghem & Botteldooren, 2011), air purification (Moghbel & Erfanian Salim, 2017), mitigation of the UHI effect (Costanzo, Evola, & Marletta, 2016; Imran, Kala, Ng, & Muthukumaran, 2018), and greater biodiversity (Brachet, Schiopu, & Clergeau, 2019). Among the multiple social, economic, and environmental benefits (Francis & Jensen, 2017), the ability of roof greening to improve microclimate has attracted substantial attention (Jim & Tsang, 2011).

While the reflectivity of GRs varies because of their different substrate types, vegetation types, and densities, GRs can shield solar radiation and mitigate heat through evapotranspiration (Zhang, Fukuda, & Liu, 2019). Moreover, more energy is partitioned into latent rather than sensible heat in locations with high annual or summer precipitation (Heusinger, Sailor, & Weber, 2018; Wong, Chen, Ong, & Sia, 2003). If enough water is available, GRs can be an effective nature-based solution for cities to adapt to climate change and to mitigate urban heat (Cartalis et al., 2001; Hoag, 2015).

Many studies have investigated the cooling mechanisms of GRs by analyzing different growth substrates (Porcaro et al., 2019), vegetation types (Huang, Chen, & Liu, 2018), irrigation (Heusinger et al., 2018; Speak, Rothwell, Lindley, & Smith, 2013), and ventilation (Gagliano, Detommaso, Nocera, & Berardi, 2016). Specifically, plant bioactivity and surface albedo play important roles in heat resistance (Susca, Gaffin, & Dell'osso, 2011). In dry and hot climates, plant growth can be maintained throughout long dry periods by using irrigation (Teemusk & Mander, 2009). Moist soil can provide heat insulation for the roof and can increase latent heat fluxes (Heusinger et al., 2018). Vegetation also functions as a “sun screen” or “shade” during the day (Peng & Yang, 2019). Denser vegetation and trees with a large leaf area index (LAI) can more effectively lower surface temperatures (Karachaliou, Santamouris, & Pangalou, 2016). Furthermore, good ventilation can alleviate high humidity caused by evapotranspiration and effectively increase the cooling effect of GRs (Gagliano et al., 2016).

As an important and widely promoted climate change adaptation measure, GRs have been implemented in many countries, while expanded research has assessed the performance of GRs in various climatic regions (Besir & Cuce, 2018). Previous performance evaluation studies can be classified as either modeling or on-site experimental studies (Santamouris, 2014). Studies based on simulations typically verify the models using in-situ observational data from the test roof, then adjust the corresponding parameters to improve the accuracy of the simulated results (Ávila-Hernández et al., 2020). Models such as ENVI-met and MM5 (Mesoscale Model 5) have been used to evaluate the impact of green spaces, buildings, and other factors on the urban thermal environment (Middel, Häb, Brazel, Martin, & Guhathakurta, 2014; Peng & Jim, 2013; Vázquez Morales et al., 2016). Previous modeling studies have reported variable cooling effects of GRs, with air temperature reductions ranging from 0.3 °C to 5.0 °C (Karachaliou et al., 2016; Peng & Jim, 2013; Rosenzweig et al., 2006; Santamouris, 2014). Improving the accuracy of numerical models remains challenging due to the complexity of the heat and mass transfer processes in GRs and the complex structure of the GR system. Therefore, observational studies are the more commonly and widely used method for investigating the cooling effects of GRs (Bevilacqua, Mazzeo, Bruno, & Arcuri, 2016; Parizotto & Lamberts, 2011).

Most experimental studies have shown that air temperature above GRs is lower than above traditional bare roofs, but the vertical cooling extent is limited to a couple of meters above the roof surface (Lilliana Peng & Jim, 2015, 2015b; Solcerova, van de Ven, Wang, Rijsdijk, & van de Giesen, 2017). Some studies have found that GRs may exhibit warming effects above the near-ground layer at specific hours during the day (Peng et al., 2019; Solcerova et al., 2017; Wong, Tan, & Chen, 2007; Yin, Kong, Dronova, Middel, & James, 2019). The vertical thermal performance characteristics and the reason for such warming effects

during the day, as well as whether this phenomenon is common or not, requires further study (Yin et al., 2019).

Previous experimental studies have often been conducted during short measurement periods at one height in small plots or modular test beds (Zhang, He, & Dewancker, 2020), which makes it difficult to extrapolate to other contexts and climatic conditions. Full-scale field observations more accurately reflect real rooftop conditions, i.e., increased exposure to wind, rain, and sun (Wolf & Lundholm, 2008). Moreover, long-term and multi-height observations can avoid interferences caused by special weather or extreme conditions, providing a more realistic reference and solid scientific data for optimizing GR function and delivery of ecosystem services to guide sustainable urban design and management. However, to date, few experimental studies have been conducted using a full-scale GR at different heights and based on long-term observations (Peng et al., 2019; Yang, Wang, Cui, Zhu, & Zhao, 2015). In particular, the vertical thermal gradient of GRs over multiple years of observation has not been thoroughly studied and remains poorly understood.

In this study, we used long-term, multi-year observational data to evaluate the outdoor thermal performance of a full-scale, sedum covered EGR in Nanjing, China and its cooling performance on multiple time scales. The aims of this study are to: (1) analyze the outdoor thermal performance of EGRs across different time scales and at different heights and (2) explore the factors that influence EGR outdoor thermal performance. The results of this study will help to promote EGRs in subtropical monsoon climates and optimize their cooling effects.

2. Materials and methods

2.1. Study area and experimental site

Nanjing (32°02'N, 118°22'E) is the capital city of Jiangsu Province, China, and has a subtropical humid climate (Köppen: Cfa) (Fig. 1(a)(b)). Nanjing has four distinct seasons: a short spring and autumn, and a long summer and winter. According to Nanjing meteorological data from 2016 to 2019, the mean annual temperature is 17 °C. In July, the maximum mean temperature is 30.8 °C and the daily maximum is 39.9 °C. The mean annual precipitation is 1160 mm, with approximately 80 % of rainfall occurring during the wet season (April to September). In the last 50 years, Nanjing has experienced rapid development; farms and forest areas have decreased in size, while built-up areas and impervious surfaces have increased rapidly (Qiu, Gu, Zeng, Jiang, & He, 2008).

The experimental site was located on the roof of the Executive Office Building at Nanjing Jinling Elementary School (JLES) in the Qixia district of Nanjing. The building is a five-story brick-concrete composite structure, with a total roof area of 1016 m². Two test areas of bare roof (BR, 507 m²) and EGR (509 m²) were implemented (Fig. 1c). Both areas were exposed to direct sunlight with no shade from other buildings around noon. The BR was composed of three layers: concrete mortar, an extruded polystyrene thermal insulation system, and a reinforced concrete roof slab (albedo of 0.29). The EGR comprised pre-grown modules containing *Sedum lineare* Thunb (Fig. 1d). The EGR was watered by hand at night on July 26, 2016 and July 29, 2016 to cope with the heat wave. Each module had a 7 cm thick soil substrate layer composed of powdered vermiculite aggregate (30 %), peat moss soil (30 %), ceramic (30 %), and organic matter (10 %); a 0.1 cm thick geotextile filter layer; and a 3.9 cm multi-functional water storage and drainage layer. *Sedum lineare* Thunb is evergreen and grows well in spring, summer, and autumn. It has a short dormancy in cold periods. For economic and practical reasons, *Sedum lineare* Thunb is considered suitable for roof greening in subtropical areas (Durham, Bradley Rowe, & Rugh, 2006; Monterusso, Rowe, & Rugh, 2005). Moreover, it is the most popular and adaptive plant for rooftops in different climatic zones (Kurokaki et al., 2015). *Sedum* species are highly reliable because they are highly tolerant to drought and shallow un-irrigated substrates. In addition, they protect against erosion from rain and provide heat insulation and cooling

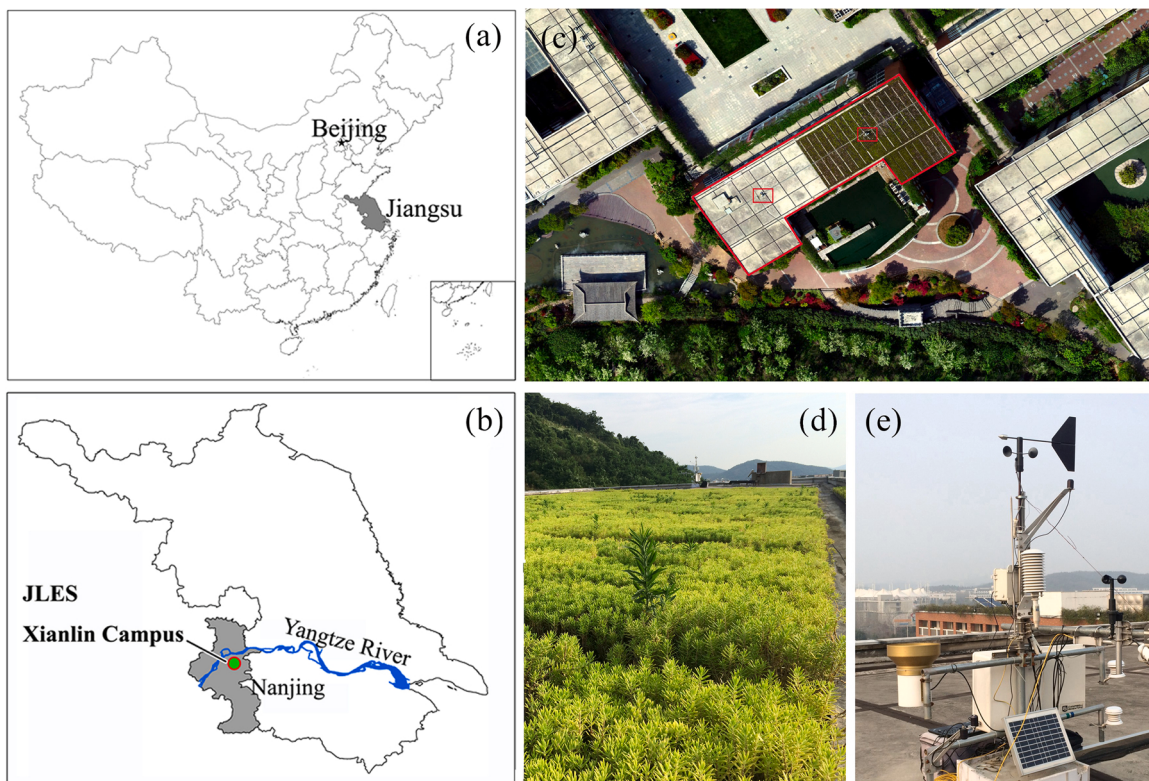


Fig. 1. (a) and (b) Maps of the study area in Nanjing, China. (c) Aerial view of the study area. (d) Photographs of *Sedum lineare* Thunb on the experimental roof during the summer, and (e) a measurement station on the bare roof.

(Dvorak & Volder, 2010).

2.2. Data sources

Roof top weather stations were installed at the center of each experimental area (Fig. 1e). Each station had one HOBO U30 (Onset Computers, Bourne, MA, USA) and one CR1000 (Campbell Scientific, Logan, UT, USA) data logger to record the air temperature (Ta), relative humidity (RH), solar radiation (SR), wind speed (WS), and net radiation (NR). The monitoring station on the EGR also had four soil temperature and moisture sensors and two soil heat flux meters, which were buried 4.5 cm deep in the substrate layer. Specific instrumental settings and parameters are shown in Table 1. The measurement period lasted from May 2016 to April 2019. All of the parameters were measured and recorded at 1 min intervals. The instruments used to measure temperature and humidity were set at heights of 30 cm, 60 cm, and 120 cm (not including the 10 cm module height).

2.3. Thermal performance analysis of extensive green roof

To ensure the accuracy of the experimental results, data were cleaned, and only continuous data were selected for further analysis.

Table 1
Instruments and variables measured in the experimental campaign.

Instrument	Sensor	Model	Parameter	Accuracy	Resolution	Installation height
HOBO U30	Temperature/RH	S-THB-M002	Temperature, relative humidity	$\pm 0.2 ^\circ\text{C}$ (0–50 °C), $\pm 2.5 \%$ (10–90 %)	0.02 °C, 0.1 %	0.3 m, 0.6 m
CR1000	Temperature/RH	HMP155A	Temperature, relative humidity	$\pm 0.1 ^\circ\text{C}$, $\pm 1 \%$	0.02 °C, 0.1 %	1.2 m
	Solar radiation	S-LIB-M003	Light intensity	$\pm 10 \text{ W/m}^2$	1.25 W/m ²	0.3 m
	Net radiometer	NR Lite2	Net radiation	<1.0 %	0.01 V/W m ⁻²	0.8 m
	Soil temperature	AV-10T	Soil temperature	$\pm 0.2 ^\circ\text{C}$ (0–70 °C)	0.01 °C	4.5 cm under soil
	Soil moisture	CS616	Soil moisture	$\pm 2.5 \%$	0.1 %	4.5 cm under soil
	Soil heat flux	HFP01	Soil heat flux	$\pm 5 \%$	0.05 V/W m ⁻²	4.5 cm under soil
	Wind speed	RM Young03001	Wind speed	$\pm 0.5 \text{ m/s}$	0.5 m/s	1.5 m

Some data loss during long-term data monitoring is unavoidable. We eliminated 11 % of the ineligible records during the data cleaning process. The remaining records were aggregated and averaged to generate hourly data.

2.3.1. Thermal performance of extensive green roof during the study period

We used observational data from May 19, 2016 to April 29, 2019 to analyze the daily temperature differences between the EGR and BR at different heights throughout the entire study period. We calculated the hourly air temperature difference (ΔT) between the EGR and BR at different heights (30 cm, 60 cm, and 120 cm):

$$\Delta T_h = T_{gh} - T_{bh} \quad (1)$$

where T_{gh} is the EGR air temperature at h cm and T_{bh} is the BR air temperature at h cm. A positive ΔT value indicates that the EGR was warmer than the BR, representing a warming effect, whereas a negative value denotes a cooling effect.

2.3.2. Diurnal thermal performance

Long-term studies of the thermal performance of GRs have reported the best cooling effects during the summer (He, Yu, Ozaki, Dong, & Zheng, 2017; Lilliana Peng & Jim, 2015). Therefore, we selected data

from July 21, 2017 to July 27, 2017 to analyze the diurnal thermal performance of the sites because this period was sunny and had high air temperatures (diurnal average of 33.9 °C), with the daily temperature ranging between 28.2 °C and 39.9 °C. The maximum temperature in 2017 was 39.9 °C, which occurred on July 24.

2.3.3. Seasonal thermal performance

We selected four months in 2017 to represent winter, spring, summer, and autumn: January 20 to February 19 (31 days), April 20 to May 19 (30 days), July 20 to August 19 (31 days), and October 20 to November 19 (31 days), respectively. These time periods were not affected by missing data. The frequency and intensity of the cooling/warming effect in the different seasons were determined by analyzing the hourly cooling/warming of the EGR during the day and at night. For T₃₀, T₆₀, and T₁₂₀, the values of the green-bare differences per unit time from 09:00 to 13:00 and from 18:00 to 23:00 were calculated to indicate the daytime warming and nighttime cooling rates, respectively.

2.3.4. Annual thermal performance

In Nanjing, August is hot and humid with occasional heavy rain. According to meteorological convention, the average temperatures at four times each day (02:00, 08:00, 14:00, and 20:00) were used to calculate the average daily temperature (Li, Miao, & He, 2013). The average temperature during August was then obtained from the daily average temperatures from August 1 to August 31. We then compared the roof's thermal performance across the three summers during the study period.

2.4. Correlation analysis

Multiple linear regression analyses were employed to explore the degree of influence of the background factors on the EGR's thermal performance. The thermal performance of GRs (and this holds for all surfaces in principle) is governed by their surface energy balances as well as the thermal properties of the materials involved including the vegetation. According to the surface energy balance equation, net radiation R_n is partitioned into sensible heat and latent heat (Peng & Yang, 2019):

$$R_n = LE + H + Q_s \quad (2)$$

where LE is the latent heat flux, H is the sensible heat flux, and Q_s is the soil heat flux.

The latent heat exchange of the plants results from evapotranspiration and is affected by WS, surface roughness, and atmospheric stability (Peng & Yang, 2019). It is widely accepted that the cooling potential of EGRs largely depends on evapotranspiration. The transpiration of plants and soil water evaporation can produce cooling effects by increasing the latent heat exchange between plants and the thermal environment; this mechanism is mostly beneficial in summer conditions (Cascone, Coma, Gagliano, & Pérez, 2019). The sensible heat exchange of plants arises from the difference in temperature between the leaf surface and the ambient air, which is affected by WS and LAI (Peng & Yang, 2019). In addition to leaf transpiration and SR absorption, shading is an important factor affecting the cooling ability of plants; the better the shading, the less heat can radiate through the plant layer (Feng, Meng, & Zhang, 2010; Kumar & Kaushik, 2005; Yang, Mohan Kumar et al., 2018).

Based on the above, we selected eight background factors (Table 2) that have the potential to influence the EGR's thermal performance. We then performed multiple linear regression analyses on these eight factors using hourly ΔT₃₀, ΔT₆₀, and ΔT₁₂₀ data from July 21 to 27, 2017 and daily daytime and nighttime data at three heights for four months in 2017. All of the calculations were conducted using SPSS (version 22). Due to correlations among the different weather variables, we selected stepwise regressions in all models, which added the independent variables one by one and only retained those that contributed significantly

Table 2

Definitions and descriptions of background factors.

No.	Name of variable	Description
1	ΔRH (%)	Relative humidity of EGR minus relative humidity of BR at the corresponding height.
2	ΔNR (Wm ⁻²)	Net radiation of EGR minus net radiation of BR.
3	ΔSR_down (Wm ⁻²)	Reflected radiation of EGR minus reflected radiation of BR.
4	SR (Wm ⁻²)	Average hourly or daily incoming solar radiation.
5	Soil_T (°C)	Arithmetic average of four soil temperature values.
6	Soil_M (m ³ /m ³)	Arithmetic average of four soil moisture values.
7	Soil_HF (Wm ⁻²)	Arithmetic average of two soil heat flux values.
8	WS (m/s)	Average hourly or daily wind speed.

to the model. Standardized coefficients were used to give indications about the relative contributions of the different factors to the thermal performance of the EGR and BR.

3. Results

3.1. Thermal performance of extensive green roof

Fig. 2 shows the daily temperature differences between the EGR and BR (ΔT₃₀, ΔT₆₀, and ΔT₁₂₀) throughout the study period. The amplitudes of ΔT at a height of 30 cm were relatively large, and the variations were higher than at the other two heights. The average ΔT₆₀ was lower than the average ΔT₃₀ and ΔT₁₂₀. According to Fig. 3 and Table 3, the ΔT₃₀ value for EGR indicates that cooling occurred on 647 days, or 75 % of the study period. More cooling days were observed at a height of 60 cm (687 out of 698 days), accounting for 98.4 % of the study period. The maximum warming effect was only 0.07 °C, whereas the maximum and average cooling effects were 0.68 °C and 0.21 °C, respectively. At a 120 cm height, 517 of 864 days (59.8 %) exhibited cooling, whereas 347 days exhibited increased temperatures. The maximum cooling effect was 0.35 °C.

In general, the average cooling values at all heights were higher than the average warming values, and the cooling days were longer than the warming days (Table 3). These results indicate an overall long-term cooling effect of the EGR, and the cooling effect was the greatest at 60 cm. The following sections present an analysis of the hourly and daily average ΔT results to determine the thermal performance of the EGR in subtropical climatic conditions on diurnal, seasonal, and annual time scales.

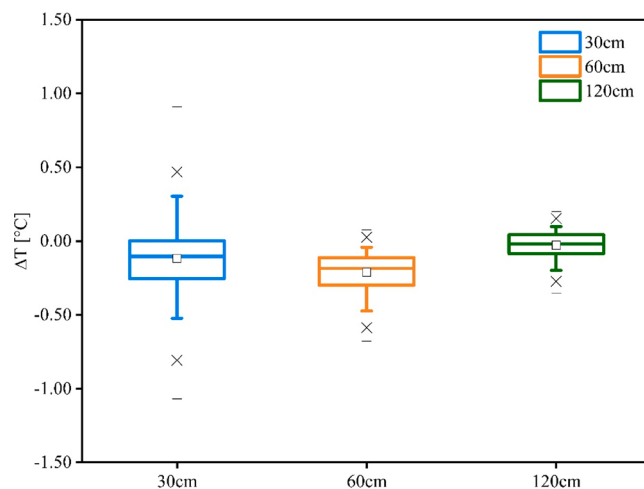


Fig. 2. ΔT statistics based on daily measurements at 30 cm, 60 cm, and 120 cm heights throughout the entire study period.

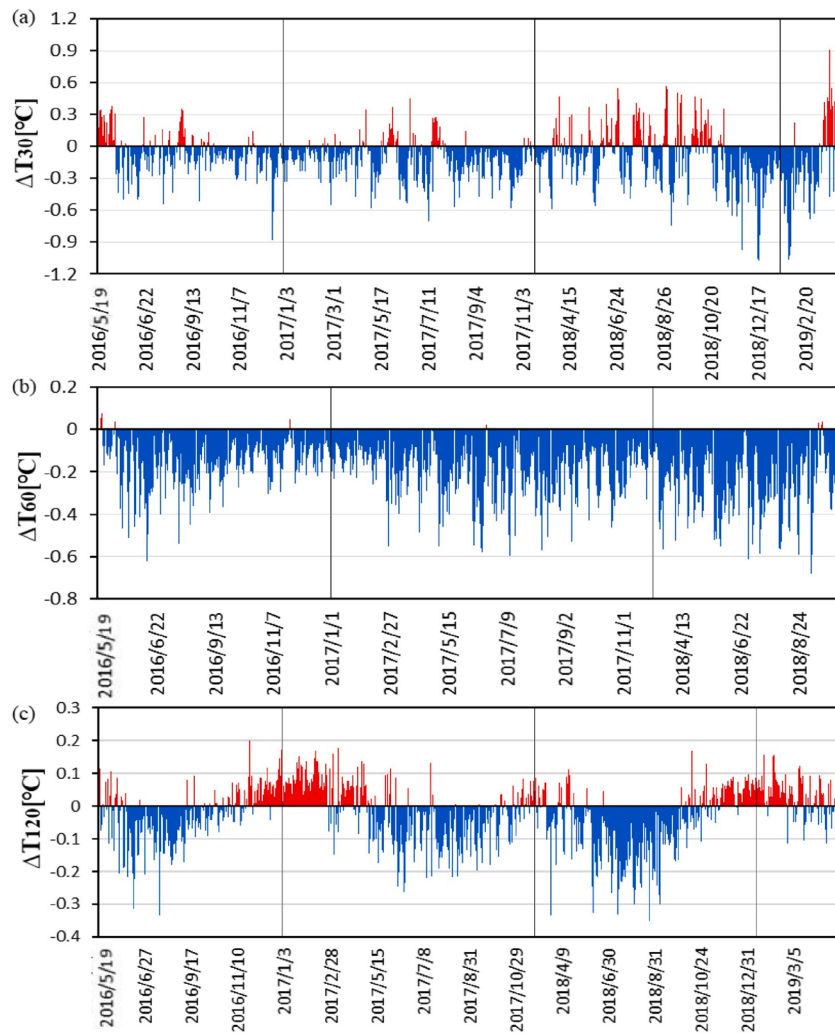


Fig. 3. Daily temperature differences between the EGR and BR throughout the study period (5/19/2016–4/29/2019): (a) air temperature differences at 30 cm (ΔT_{30}), (b) air temperature differences at 60 cm (ΔT_{60}), (c) air temperature differences at 120 cm (ΔT_{120}). Missing data and outliers have been removed.

Table 3

Summary of the daily thermal performance of the EGR at three heights.

Height (cm)	$\Delta T < 0 {^{\circ}\text{C}}$			$\Delta T \geq 0 {^{\circ}\text{C}}$			Total	
	Days	Min ($^{\circ}\text{C}$)	Mean ($^{\circ}\text{C}$)	Days	Max ($^{\circ}\text{C}$)	Mean ($^{\circ}\text{C}$)	Days	SD
30	647	-1.07	-0.22	216	0.91	0.17	863	0.24
60	687	-0.68	-0.21	11	0.07	0.03	698	0.13
120	517	-0.35	-0.09	347	0.20	0.06	864	0.09

Note: Only valid data are shown. Min = minimum; Max = maximum; SD = standard deviation.

3.2. Diurnal patterns of extensive green roof thermal performance

Fig. 4 shows the hourly air temperature differences between the EGR and BR at all three heights from July 21 to July 27, 2017 (the selected summer period). Due to clear days, temperature was not affected by precipitation. The EGR displayed similar cooling/warming trends at all heights. The 30 cm air temperature was higher on the EGR compared to the BR from approximately 07:00 to 16:00, and the maximum warming amplitude was 2.89 $^{\circ}\text{C}$ (July 24, 11:00). The cooling effect of the EGR was observed from 17:00 to 06:00, with a maximum temperature decreased of 1.63 $^{\circ}\text{C}$ (July 23, 23:00). At 60 cm, the EGR generally exhibited a warming effect from 07:00 to 15:00 (July 21–25); however, the EGR was cooler than the BR during the remaining hours. Conversely, on July 26 and July 27, a weak warming effect was only observed for 2 h

each day, with a maximum warming of 0.80 $^{\circ}\text{C}$ (July 24, 11:00) but a maximum cooling of 1.31 $^{\circ}\text{C}$ (July 23, 22:00). At 120 cm, a warming effect generally occurred from 07:00 to 15:00 from July 21 to July 25, with the temperature of the EGR lower than that of the BR during the remaining hours. Conversely, on July 26 and July 27, only one hour of warming occurred each day with an extremely low warming magnitude; the maximum warming was 0.86 $^{\circ}\text{C}$ (July 24, 11:00) and the maximum cooling was 0.75 $^{\circ}\text{C}$ (July 22, 23:00). Therefore, the EGR did not reduce the ambient air temperature at all times, and a period of warming occurred during the daytime. Both the warming and cooling effects were stronger closer to the surface of the EGR.

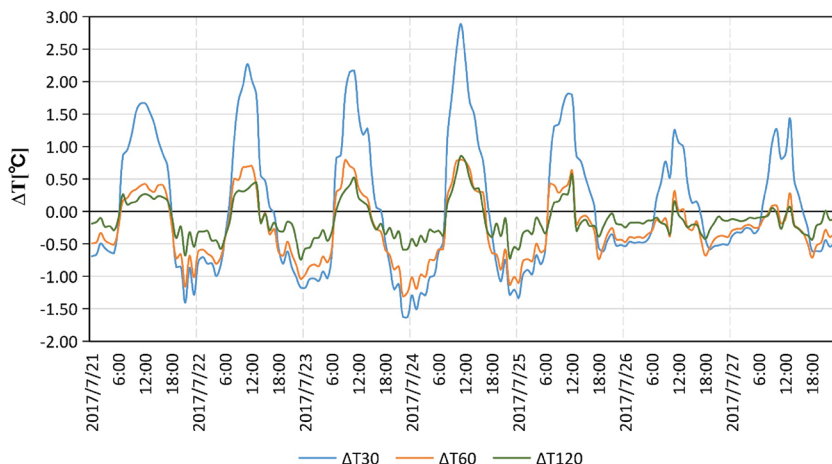


Fig. 4. Hourly differences in air temperature between the EGR and BR at heights of 30 cm, 60 cm, and 120 cm during the selected summer period (July 21 to July 27, 2017).

3.3. Seasonal patterns of extensive green roof thermal performance

The cooling effect of the EGR exhibited subtle seasonal differences at different heights (Table 4). The EGR had a greater cooling effect at 60 cm than at 30 cm or 120 cm. The average cooling effect at 60 cm during the winter, spring, summer, and autumn was 0.14 °C, 0.26 °C, 0.28 °C, and 0.21 °C, respectively; the cooling effect was largest in the summer, although the results are within sensor accuracy. The range of temperature changes was greater at 30 cm than at the other two heights, and the temperature variations were greater in the summer than in the other three seasons. These findings demonstrate the following: (1) at 30 cm, the EGR caused a maximum temperature decrease of 1.86 °C (winter and summer) and an increase of 2.89 °C (summer); (2) at 60 cm, the EGR caused a maximum temperature decrease of only 1.39 °C (summer) and an increase of 0.86 °C (summer). Between January 20 and February 19, the average temperature difference between the EGR and BR at 120 cm was 0.08 °C, indicating that the EGR had a negligible warming effect during the winter. The mean temperature differences between the EGR and BR from 09:00 to 13:00 and from 18:00 to 23:00 were calculated to indicate the daytime warming and nighttime hourly cooling rates, respectively (Fig. 5).

3.3.1. Daytime and nighttime temperatures at 30 cm height (DT_{30} and NT_{30})

Compared with T_{60} and T_{120} , T_{30} is the temperature closest to the roof surface and can accurately reflect the difference in temperature between roofs with and without vegetation after exposure to SR. Among the 123 days of recorded data, the EGR exhibited daytime warming on 109 days (88.6 %), which were evenly distributed among the four

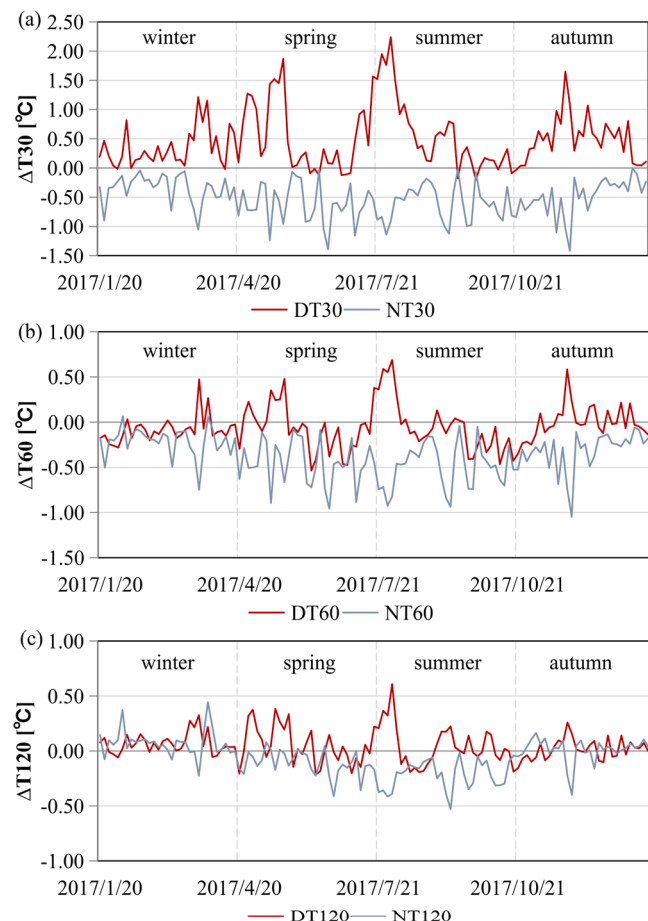


Fig. 5. Daily average EGR cooling and warming rates of ambient air during the four seasons: (a) 30 cm (T_{30}), (b) 60 cm (T_{60}), and (c) 120 cm (T_{120}). DT and NT represent warming (positive values) or cooling (negative values) rates during the daytime and nighttime, respectively.

seasons. The average daily warming was the highest during the summer (0.7 °C), with the maximum daily warming occurring on July 24 (2.23 °C). The average daily warming in spring, autumn, and winter was 0.65 °C, 0.52 °C, and 0.38 °C, respectively. Nighttime cooling occurred every day at a height of 30 cm. Although the daily cooling intensity varied, the average cooling during spring, summer, and autumn was 0.62 °C, 0.59

Note: Min = minimum; Max = maximum; SD = standard deviation.

°C, and 0.50 °C, respectively, indicating no significant differences. The minimum cooling (0.34 °C) occurred in the winter, while the maximum cooling (1.41 °C) occurred in the autumn (November 2).

3.3.2. Daytime and nighttime temperatures at 60 cm height (DT_{60} and NT_{60})

The temperatures measured at 60 cm above the ground indicate that the main influences of the EGR on the ambient temperature was daytime cooling (91 days) and nighttime cooling (121 days). The temperature increase was less than at 30 cm height. Only two nighttime warming events occurred during the winter, whereas daytime warming was distributed across the four seasons: eight days in the spring, ten days in the summer and autumn, and four days in the winter. The maximum temperature increase was 0.68 °C in the summer (July 24). Overall, the EGR had a much smaller effect on air temperatures in the winter than in the summer.

3.3.3. Daytime and nighttime temperatures at 120 cm height (DT_{120} and NT_{120})

The 120 cm air temperatures were the closest to the atmospheric temperatures on the ground and were minimally influenced by the EGR, as shown by very small cooling and warming amplitudes. The thermal performance of the EGR at 120 cm differed from that at 30 cm and 60 cm. The EGR exhibited a daytime warming effect on 71 days, with the majority occurring in the winter (25 days). During the other seasons, warming was evenly distributed and more daytime cooling occurred. The maximum daily temperature also decreased in the summer and 71 days exhibited nighttime cooling, 78.9 % of which occurred in spring and summer, with a maximum decrease of 0.53 °C (August 6). In autumn and winter, nighttime warming was the most obvious phenomenon. The maximum temperature increase at night (0.37 °C) also occurred in the winter (January 25). Therefore, the thermal performance of the EGR at 120 cm was predominantly characterized by increased air temperatures in the winter and a dominant cooling effect in the summer.

3.4. Annual patterns of extensive green roof thermal performance

A comparison of the cooling effect of the EGR in 2016, 2017, and 2018 (August 1 to August 31) indicates that the EGR can reduce air temperatures during the summer to a limited extent. The EGR exhibited a better cooling effect at a 60 cm height (Fig. 6). The weaker average cooling effect at 120 cm was due to the greater distance from the roof surface and the reduced influence of plants. However, the EGR exhibited a good cooling effect in August 2018, when cooling at 60 cm and 120 cm were slightly stronger than in 2016 and 2017, indicating that the cooling effect of EGRs is sustainable.

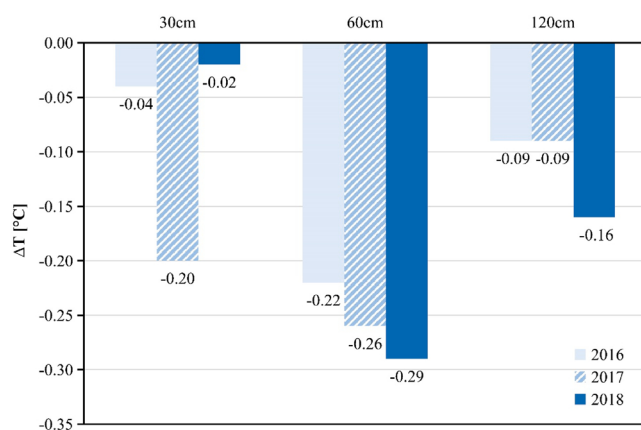


Fig. 6. Average air temperature reductions due to the EGR at heights of 30 cm, 60 cm, and 120 cm in August 2016, 2017, and 2018.

3.5. Factors influencing extensive green roof thermal performance

Multiple linear regression analyses were performed to determine the notable impacts of background weather factors on the EGR's thermal performance (Table 5). Different variables were selected in different specific models. For example, the average measurement value based on daily data can only represent the daily variation in different factors. Moreover, some factors that change continuously throughout the day are not reflected by the daily average value, such as WS and SR. Therefore, the thermal performance of the EGR on different time scales was attributed to different factors. The adjusted R^2 values for the regression of the dependent variables ΔT_{30} , ΔT_{60} , and ΔT_{120} were 0.978, 0.980, and 0.941, respectively. Thus, the fitting degree of the regression equations was extremely high. The RH at the corresponding height typically exhibited significant correlations with the highest correlation coefficients. RH was negatively correlated with hourly ΔT , suggesting that the higher the RH of the EGR, the greater the cooling effect. High RH always corresponds to low SR (Theodosiou, 2003), which suppresses EGR warming. However, a high RH at night will reduce the evaporation from plants, thereby weakening the cooling effect (Jim & Tsang, 2011).

NR and SR played dominant roles in regulating EGR thermal performance. They exhibited the same number of significant correlations but were correlated differently with thermal indicators and reliability coefficients. The intensity of SR determines the heat storage, surface temperature, and thermal balance of roofs (Tabares-Velasco & Srebric, 2012). SR was positively correlated with DT and negatively correlated with NT. Compared to SR, SR_{down} was more significantly and negatively correlated with ΔT ; therefore, the stronger the SR reflected by the EGR, the better the cooling effect.

Three variables related to the soil (soil temperature, soil moisture, and soil heat flux) were monitored in this study. As July 21 to July 27, 2017 was characterized by continuously high daytime temperatures and sunny days, there was no rainfall, resulting in the soil drying out and almost no changes in the soil water content. Therefore, no correlation was observed between ΔT and soil moisture during this period, as shown by the stepwise regression analyses. The results present a negative correlation between thermal indicators and soil moisture, but a positive correlation with soil heat flux.

WS exhibited the greatest number of significant correlations with the thermal indicators, although the correlation coefficients were typically low. A positive correlation was observed between WS and NT, whereas all other correlations were negative.

4. Discussion

GRs are effective measures for urban microclimate regulation that can reduce energy consumption for air conditioning and reduce outdoor air temperature in cities, thus alleviating the UHI effect. EGRs are popular GRs due to their low installation and maintenance costs. The EGR monitored in this study exhibited different cooling characteristics across multiple time scales, which were influenced by various environmental factors. Surprisingly, the diurnal pattern of the EGR's thermal performance was characterized by warming during the daytime. During periods of continuous high temperatures and sunny days, the EGR produced a cooling effect between at least 16:00 and 06:00 the next day, whereas the warming effect typically peaked at noon. In contrast, previous studies have reported good cooling effects of GRs on the surrounding environment during the summer (Alexandri & Jones, 2008). According to Rosenzweig et al. (2006), who simulated GRs with an equivalent albedo of 0.8, the use of GRs provides an important cooling impact in cities. In contrast, some recent experiments have revealed that GRs do not always exhibit a cooling effect and can be warmer than traditional roofs during the day (Peng et al., 2019; Wong et al., 2007; Yin et al., 2019). Different factors have been proposed to explain the warming effect observed on sunny days (Karachaliou et al., 2016; Solcerova et al., 2017), such as the exposure of bare soil due to incomplete

Table 5
Results of multiple linear stepwise regression analyses.

Background factor/ thermal indicator	ΔT_{30}	ΔT_{60}	ΔT_{120}	DT_{30}	NT_{30}	DT_{60}	NT_{60}	DT_{120}	NT_{120}
Adjusted R ²	0.978	0.980	0.941	0.733	0.634	0.566	0.667	0.106	0.585
Constant	-0.070	0.388	0.411	0.605	-0.219	0.255	-0.190	0.045	0.197
ΔRH	-0.299** (-0.881)	-0.319** (-0.764)	-0.282** (-0.847)	-	-0.110** (-0.271)	-	-0.203** (-0.478)	-	-0.092** (-0.280)
ΔNR	-0.012** (-0.240)	-0.009** (-0.391)	-0.007** (-0.498)	-0.014** (-0.349)	-	-0.009** (-0.533)	-	-	-
ΔSR_{down}	-0.032** (-0.290)	-0.009** (-0.170)	-0.010** (-0.340)	0.013* (0.149)	-	0.010** (0.267)	-0.007** (-0.180)	-	-
SR	0.001** (0.145)	-	-	0.005** (0.647)	-0.003** (-0.652)	0.001** (0.393)	-0.001** (-0.321)	-	-
Soil_T	0.013** (0.116)	-	-	-	-	-	-	-	-0.009** (-0.667)
Soil_M	-	-	-	-2.569** (-0.287)	-	-1.201** (-0.297)	-	-	-0.553* (-0.174)
Soil_HF	-	0.005** (0.197)	0.003** (0.207)	0.020* (0.166)	-	-	-	0.010** (0.337)	-
WS	-0.048* (-0.038)	-0.036** (-0.060)	-0.044** (-0.124)	-0.271** (-0.333)	0.180** (0.354)	-0.159** (-0.432)	0.117** (0.296)	-	-

Note: ΔT_{30} , ΔT_{60} , ΔT_{120} , and corresponding background factors were based on hourly data. Background factors for DT and NT were based on daily data. Beta values in parentheses are standardized coefficients.

* Correlation is significant at the 0.05 level (two-tailed).

** Correlation is significant at the 0.01 level (two-tailed).

vegetation coverage. In addition, the vegetated EGR had a lower albedo than the grayish-white BR, and the Sedum species close their stomata on hot days for water conservation, which stops evapotranspiration. The timing and magnitude of the cooling effect is also dependent on the type of the reference roof and its thermal and radiative properties, which should be studied further. The specific mechanism likely involves many factors, leading to variable results obtained by various studies. Hence, further experimental research is required to better understand these factors and the mechanisms involved.

A significant positive correlation was observed between DT_{30} and SR, whereas a negative correlation was observed between DT_{30} and soil moisture. It is reasonable to infer that insufficient soil water content inhibited adequate evaporation and led to higher surface roughness, which can trap heat and water within the near-surface boundary layer (Cascone et al., 2019). When the canopy resistance is high, the water that moves toward the leaf surface does not easily evaporate (Solcerova et al., 2017).

One of the reasons for the formation of the UHI effect is that, after an impervious surface absorbs SR, more radiant heat is emitted to the surrounding areas, leading to an increase in air temperature (Guo et al., 2019). Thus, the cooling effects of GRs have the potential to significantly mitigate UHI effects. Yang, Mohan Kumar et al. (2018) and Yang, Yao et al. (2018) found that UHIs in Nanjing typically occur at night, from sunset until two hours after sunrise the next morning, which corresponds to the timing of the EGR's cooling effect observed in this study.

Soil temperature, moisture, and heat flux are related to the EGR thermal performance. Soil thermal properties are determined by many factors, one of which is soil moisture (Azeñas et al., 2018). Soil moisture also determines the water available for evapotranspiration and latent heat exchange. However, water can increase the soil thermal conductivity, which can then increase the heat transfer to the building (Jim & Peng, 2012). Moreover, the heat fluxes of different soil types differ, even under the same conditions (Oliver, Oliver, Wallace, & Roberts, 1987), which affects the cooling impact of EGRs. Therefore, previous studies have compared the cooling effects of GRs with different substrates (Porcaro et al., 2019).

WS affects the heat transfer coefficient between the surface and the atmosphere (Kolokotroni, Gowreesunker, & Giridharan, 2013). Jiang and Tang (2017) studied the effect of nighttime ventilation on the cooling effect of GRs and showed that combining GRs and nighttime ventilation can significantly reduce air temperatures above the roof on

sunny days. Moreover, wind can enhance evapotranspiration-related cooling and can facilitate advection, resulting in cooling of the surrounding environment (Peng et al., 2019).

The cooling effect was weaker near the roof and furthest from the top of the roof. This is similar to the findings of Wong et al. (2003), who illustrated that the influence of plants on the microclimate occurred within a height of 70 cm from the plants. In the daytime, the surrounding temperature was higher closer to the rooftop because the intense SR raised the surface temperature, thereby affecting the surrounding air temperature, which gradually decreased with increasing height. The temperature curve at night exhibited the opposite pattern.

While we investigated the thermal performance of an EGR across multiple time scales in a longitudinal study, we did not assess the influence of various plants at different growth stages. Future studies should also investigate the cooling effect of GRs under different climatic conditions.

5. Conclusions

The thermal performance of an EGR in a subtropical climate was studied using three years (2016, 2017, and 2018) of observational data from Nanjing, China, to determine the cooling effect of GRs. The thermal performance of the EGR demonstrated notable diurnal, seasonal, and annual patterns. A temporary warming effect was observed during the day, especially around midday, while cooling effects were more pronounced at night. The most pronounced cooling effect occurred at a height of 60 cm. The EGR had the most significant cooling influence on air temperatures in the summer, as well as slight warming effects in the winter at a height of 120 cm.

Multiple stepwise regression analyses showed that factors such as SR, RH, WS, and soil substrate layer played a role in EGR cooling and were important drivers of the thermal performance of the EGR across time scales. This study suggests that EGRs can improve outdoor thermal conditions and mitigate the UHI effect, providing a new method for enhancing the sustainability of urban developments in subtropical climates.

Declaration of Competing Interest

The authors report no declarations of interest.

Acknowledgements

This research was supported by the National Key R&D Program of China (No. 2017YFE0196000), and the National Natural Science Foundation of China (Nos. 51878328 and 31670470).

References

- Alexandri, E., & Jones, P. (2008). Temperature decreases in an urban canyon due to green walls and green roofs in diverse climates. *Building and Environment*, 43, 480–493. <https://doi.org/10.1016/j.buildenv.2006.10.055>
- Ávila-Hernández, A., Simá, E., Xamán, J., Hernández-Pérez, I., Téllez-Velázquez, E., & Chagolla-Aranda, M. A. (2020). Test box experiment and simulations of a green-roof: Thermal and energy performance of a residential building standard for Mexico. *Energy and Buildings*, 209. <https://doi.org/10.1016/j.enbuild.2019.109709>
- Azenas, V., Cuxart, J., Picos, R., Medrano, H., Simó, G., López-Grifol, A., et al. (2018). Thermal regulation capacity of a green roof system in the mediterranean region: The effects of vegetation and irrigation level. *Energy and Buildings*, 164, 226–238. <https://doi.org/10.1016/j.enbuild.2018.01.010>
- Barnhart, B., Pettus, P., Halama, J., McKane, R., Mayer, P., Djang, K., ... Moskal, L. M. (2021). Modeling the hydrologic effects of watershed-scale green roof implementation in the Pacific Northwest, United States. *Journal of Environmental Management*, 277, Article 111418. <https://doi.org/10.1016/j.jenvman.2020.111418>
- Besir, A. B., & Cuce, E. (2018). Green roofs and facades: A comprehensive review. *Renewable and Sustainable Energy Reviews*, 82, 915–939. <https://doi.org/10.1016/j.rser.2017.09.106>
- Bevilacqua, P., Mazzeo, D., Bruno, R., & Arcuri, N. (2016). Experimental investigation of the thermal performances of an extensive green roof in the Mediterranean area. *Energy and Buildings*, 122, 63–79. <https://doi.org/10.1016/j.enbuild.2016.03.062>
- Brachet, A., Schiopu, N., & Clergeau, P. (2019). Biodiversity impact assessment of building's roofs based on Life Cycle Assessment methods. *Building and Environment*, 158, 133–144. <https://doi.org/10.1016/j.buildenv.2019.04.014>
- Cartalis, C., Synodinou, A., Proedrou, M., Tsangrassoulis, A., & Santamouris, M. (2001). Modifications in energy demand in urban areas as a result of climate changes: An assessment for the southeast Mediterranean region. *Energy Conversion and Management*, 42, 1647–1656. [https://doi.org/10.1016/s0196-8904\(00\)00156-4](https://doi.org/10.1016/s0196-8904(00)00156-4)
- Cascone, S., Coma, J., Gagliano, A., & Pérez, G. (2019). The evapotranspiration process in green roofs: A review. *Building and Environment*, 147, 337–355. <https://doi.org/10.1016/j.buildenv.2018.10.024>
- Castleton, H. F., Stovin, V., Beck, S. B. M., & Davison, J. B. (2010). Green roofs; building energy savings and the potential for retrofit. *Energy and Buildings*, 42, 1582–1591. <https://doi.org/10.1016/j.enbuild.2010.05.004>
- Costanzo, V., Evola, G., & Marletta, L. (2016). Energy savings in buildings or UHI mitigation? Comparison between green roofs and cool roofs. *Energy and Buildings*, 114, 247–255. <https://doi.org/10.1016/j.enbuild.2015.04.053>
- Durhman, A. K., Bradley Rowe, D., & Rugh, C. L. (2006). Effect of watering regimen on chlorophyll fluorescence and growth of selected green roof plant taxa. *HortScience*, 41, 1623–1628. <https://doi.org/10.21273/horts.41.7.1623>
- Dvorak, B., & Volder, A. (2010). Green roof vegetation for North American ecoregions: A literature review. *Landscape and Urban Planning*, 96, 197–213. <https://doi.org/10.1016/j.landurbplan.2010.04.009>
- Feng, C., Meng, Q., & Zhang, Y. (2010). Theoretical and experimental analysis of the energy balance of extensive green roofs. *Energy and Buildings*, 42, 959–965. <https://doi.org/10.1016/j.enbuild.2009.12.014>
- Francis, L. F. M., & Jensen, M. B. (2017). Benefits of green roofs: A systematic review of the evidence for three ecosystem services. *Urban Forestry & Urban Greening*, 28, 167–176. <https://doi.org/10.1016/j.ufug.2017.10.015>
- Gagliano, A., Detommaso, M., Nocera, F., & Berardi, U. (2016). The adoption of green roofs for the retrofitting of existing buildings in the Mediterranean climate. *International Journal of Sustainable Building Technology and Urban Development*, 7, 116–129. <https://doi.org/10.1080/2093761x.2016.1172279>
- Guo, L., Liu, R., Men, C., Wang, Q., Miao, Y., & Zhang, Y. (2019). Quantifying and simulating landscape composition and pattern impacts on land surface temperature: A decadal study of the rapidly urbanizing city of Beijing, China. *The Science of the Total Environment*, 654, 430–440. <https://doi.org/10.1016/j.scitotenv.2018.11.108>
- Hallegatte, S., & Corfee-Morlot, J. (2010). Understanding climate change impacts, vulnerability and adaptation at city scale: An introduction. *Climatic Change*, 104, 1–12. <https://doi.org/10.1007/s10584-010-9981-8>
- He, Y., Yu, H., Ozaki, A., Dong, N., & Zheng, S. (2017). Long-term thermal performance evaluation of green roof system based on two new indexes: A case study in Shanghai area. *Building and Environment*, 120, 13–28. <https://doi.org/10.1016/j.buildenv.2017.04.001>
- Heusinger, J., & Weber, S. (2017). Surface energy balance of an extensive green roof as quantified by full year eddy-covariance measurements. *The Science of the Total Environment*, 577, 220–230. <https://doi.org/10.1016/j.scitotenv.2016.10.168>
- Heusinger, J., Sailor, D. J., & Weber, S. (2018). Modeling the reduction of urban excess heat by green roofs with respect to different irrigation scenarios. *Building and Environment*, 131, 174–183. <https://doi.org/10.1016/j.buildenv.2018.01.003>
- Hoag, H. (2015). How cities can beat the heat. *Nature*, 524, 402–404. <https://doi.org/10.1038/524402a>
- Hoffman, L., & McDonough, W. (2005). *Green roofs: Ecological design and construction*. Schiffer Publishing.
- Huang, Y.-Y., Chen, C.-T., & Liu, W.-T. (2018). Thermal performance of extensive green roofs in a subtropical metropolitan area. *Energy and Buildings*, 159, 39–53. <https://doi.org/10.1016/j.enbuild.2017.10.039>
- Imran, H. M., Kala, J., Ng, A. W. M., & Muthukumaran, S. (2018). Effectiveness of green and cool roofs in mitigating urban heat island effects during a heatwave event in the city of Melbourne in southeast Australia. *Journal of Cleaner Production*, 197, 393–405. <https://doi.org/10.1016/j.jclepro.2018.06.179>
- Jiang, L., & Tang, M. (2017). Thermal analysis of extensive green roofs combined with night ventilation for space cooling. *Energy and Buildings*, 156, 238–249. <https://doi.org/10.1016/j.enbuild.2017.09.080>
- Jim, C. Y., & Peng, L. H. (2012). Substrate moisture effect on water balance and thermal regime of a tropical extensive green roof. *Ecological Engineering*, 47, 9–23. <https://doi.org/10.1016/j.ecoleng.2012.06.020>
- Jim, C. Y., & Tsang, S. W. (2011). Ecological energetics of tropical intensive green roof. *Energy and Buildings*, 43, 2696–2704. <https://doi.org/10.1016/j.enbuild.2011.06.018>
- Karachalios, P., Santamouris, M., & Pangalou, H. (2016). Experimental and numerical analysis of the energy performance of a large scale intensive green roof system installed on an office building in Athens. *Energy and Buildings*, 114, 256–264. <https://doi.org/10.1016/j.enbuild.2015.04.055>
- Kolokotroni, M., Gowreesunker, B. L., & Giridharan, R. (2013). Cool roof technology in London: An experimental and modelling study. *Energy and Buildings*, 67, 658–667. <https://doi.org/10.1016/j.enbuild.2011.07.011>
- Kong, F., Sun, C., Liu, F., Yin, H., Jiang, F., Pu, Y., Cavan, G., Skelhorn, C., Middel, A., & Drnová, I. (2016). Energy saving potential of fragmented green spaces due to their temperature regulating ecosystem services in the summer. *Applied Energy*, 183, 1428–1440. <https://doi.org/10.1016/j.apenergy.2016.09.070>
- Kumar, R., & Kaushik, S. C. (2005). Performance evaluation of green roof and shading for thermal protection of buildings. *Building and Environment*, 40, 1505–1511. <https://doi.org/10.1016/j.buildenv.2004.11.015>
- Kurosaki, K., Umeda, A., Kumagai, M., Ohishi, Y., Muta, H., & Yamamoto, S. (2015). Microstructure and Thermal Conductivity of RuAl₂ Prepared by a Single-Roll Melting Spinning Method. *Journal of the Japan Institute of Metals*, 79, 573–576. <https://doi.org/10.2320/jinstmet.JA201502>
- Li, Y., Miao, J., & He, Y. (2013). Influence of calculation methods on calculated daily mean temperature. *Meteorological science and technology*, 41, 88–92. <https://doi.org/10.3969/j.issn.1671-6345.2013.01.017>
- Peng, L., & Jim, C. (2015). Seasonal and diurnal thermal performance of a subtropical extensive green roof: The impacts of background weather parameters. *Sustainability*, 7, 11098–11113. <https://doi.org/10.3390/su70811098>
- Peng, L. H., & Jim, C. Y. (2015). Economic evaluation of green-roof environmental benefits in the context of climate change: The case of Hong Kong. *Urban Forestry & Urban Greening*, 14, 554–561. <https://doi.org/10.1016/j.ufug.2015.05.006>
- Mathieu, R., Freeman, C., & Aryal, J. (2007). Mapping private gardens in urban areas using object-oriented techniques and very high-resolution satellite imagery. *Landscape and Urban Planning*, 81, 179–192. <https://doi.org/10.1016/j.landurbplan.2006.11.009>
- Middel, A., Häb, K., Brazel, A. J., Martin, C. A., & Guhathakurta, S. (2014). Impact of urban form and design on mid-afternoon microclimate in Phoenix local Climate Zones. *Landscape and Urban Planning*, 122, 16–28. <https://doi.org/10.1016/j.landurbplan.2013.11.004>
- Moghbel, M., & Erfanian Salim, R. (2017). Environmental benefits of green roofs on microclimate of Tehran with specific focus on air temperature, humidity and CO₂ content. *Urban Climate*, 20, 46–58. <https://doi.org/10.1016/j.ulclim.2017.02.012>
- Monterusso, M., Rowe, D., & Rugh, C. (2005). Establishment and persistence of *Sedum* spp. and native taxa for green roof applications. *HortScience*, 40(2), 391–396.
- Ng, E., Chen, L., Wang, Y., & Yuan, C. (2012). A study on the cooling effects of greening in a high-density city: An experience from Hong Kong. *Building and Environment*, 47, 256–271. <https://doi.org/10.1016/j.buildenv.2011.07.014>
- Oliver, S. A., Oliver, H. R., Wallace, J. S., & Roberts, A. M. (1987). Soil heat flux and temperature variation with vegetation, soil type and climate. *Agricultural and Forest Meteorology*, 39, 257–269. [https://doi.org/10.1016/0168-1923\(87\)90042-6](https://doi.org/10.1016/0168-1923(87)90042-6)
- Parizotto, S., & Lamberts, R. (2011). Investigation of green roof thermal performance in temperate climate: A case study of an experimental building in Florianópolis city, Southern Brazil. *Energy and Buildings*, 43, 1712–1722. <https://doi.org/10.1016/j.enbuild.2011.03.014>
- Peng, L., & Jim, C. (2013). Green-roof effects on neighborhood microclimate and human thermal sensation. *Energies*, 6, 598–618. <https://doi.org/10.3390/en6020598>
- Peng, M.-x., & Yang, Z.-j. (2019). Cooling and humidification effect of green roof on the outdoor microclimate. *Journal of Civil & Environmental Engineering*, 41, 165–173. <https://doi.org/10.11835/j.issn.2096-6717.2019.085>
- Peng, L. L. H., Yang, X., He, Y., Hu, Z., Xu, T., Jiang, Z., et al. (2019). Thermal and energy performance of two distinct green roofs: Temporal pattern and underlying factors in a subtropical climate. *Energy and Buildings*, 185, 247–258. <https://doi.org/10.1016/j.enbuild.2018.12.040>
- Porcaro, M., de Adana, M. R., Comino, F., Peña, A., Martín-Conseguera, E., & Vanwallegem, T. (2019). Long term experimental analysis of thermal performance of extensive green roofs with different substrates in Mediterranean climate. *Energy and Buildings*, 197, 18–33. <https://doi.org/10.1016/j.enbuild.2019.05.041>
- Qiu, X. F., Gu, L. H., Zeng, Y., Jiang, A. J., & He, Y. J. (2008). Study on urban heat island effect of Nanjing. *Climatic and Environmental Research*, 13, 807–814.
- Rosenzweig, C., Solecki, W., Parshall, L., Gaffin, S., Lynn, B., Goldberg, R., Cox, J., & Hodges, S. (2006). Mitigating New York City's heat island with urban forestry, living roofs, and light surfaces. *86th AMS Annual Meeting*.
- Santamouris, M. (2014). Cooling the cities – A review of reflective and green roof mitigation technologies to fight heat island and improve comfort in urban

- environments. *Solar Energy*, 103, 682–703. <https://doi.org/10.1016/j.solener.2012.07.003>
- Santamouris, M. (2015). Regulating the damaged thermostat of the cities—Status, impacts and mitigation challenges. *Energy and Buildings*, 91, 43–56. <https://doi.org/10.1016/j.enbuild.2015.01.027>
- Solcerova, A., van de Ven, F., Wang, M., Rijssdijk, M., & van de Giesen, N. (2017). Do green roofs cool the air? *Building and Environment*, 111, 249–255. <https://doi.org/10.1016/j.buildenv.2016.10.021>
- Speak, A. F., Rothwell, J. J., Lindley, S. J., & Smith, C. L. (2013). Reduction of the urban cooling effects of an intensive green roof due to vegetation damage. *Urban Climate*, 3, 40–55. <https://doi.org/10.1016/j.uclim.2013.01.001>
- Susca, T., Gaffin, S. R., & Dell'osso, G. R. (2011). Positive effects of vegetation: Urban heat island and green roofs. *Environ Pollut*, 159, 2119–2126. <https://doi.org/10.1016/j.envpol.2011.03.007>
- Tabares-Velasco, P. C., & Srebric, J. (2012). A heat transfer model for assessment of plant based roofing systems in summer conditions. *Building and Environment*, 49, 310–323. <https://doi.org/10.1016/j.buildenv.2011.07.019>
- Teemusk, A., & Mander, Ü. (2009). Greenroof potential to reduce temperature fluctuations of a roof membrane: A case study from Estonia. *Building and Environment*, 44, 643–650. <https://doi.org/10.1016/j.buildenv.2008.05.011>
- Theodosiou, T. G. (2003). Summer period analysis of the performance of a planted roof as a passive cooling technique. *Energy and Buildings*, 35, 909–917. [https://doi.org/10.1016/s0378-7788\(03\)00023-9](https://doi.org/10.1016/s0378-7788(03)00023-9)
- Van Renterghem, T., & Botteldooren, D. (2011). In-situ measurements of sound propagating over extensive green roofs. *Building and Environment*, 46, 729–738. <https://doi.org/10.1016/j.buildenv.2010.10.006>
- Vázquez Morales, W., Jazcilevich, A., Reynoso, A. G., Caetano, E., Gómez, G., & Bornstein, R. D. (2016). Influence of green roofs on early morning mixing layer depths in Mexico City. *Journal of Solar Energy Engineering*, 138. <https://doi.org/10.1115/1.4034807>
- Wang, X., Tian, Y., & Zhao, X. (2017). The influence of dual-substrate-layer extensive green roofs on rainwater runoff quantity and quality. *The Science of the Total Environment*, 592, 465–476. <https://doi.org/10.1016/j.scitotenv.2017.03.124>
- Wolf, D., & Lundholm, J. T. (2008). Water uptake in green roof microcosms: Effects of plant species and water availability. *Ecological Engineering*, 33, 179–186. <https://doi.org/10.1016/j.ecoleng.2008.02.008>
- Wong, N. H., Chen, Y., Ong, C. L., & Sia, A. (2003). Investigation of thermal benefits of rooftop garden in the tropical environment. *Building and Environment*, 38, 261–270. [https://doi.org/10.1016/s0360-1323\(02\)00066-5](https://doi.org/10.1016/s0360-1323(02)00066-5)
- Wong, N. H., Tan, P. Y., & Chen, Y. (2007). Study of thermal performance of extensive rooftop greenery systems in the tropical climate. *Building and Environment*, 42, 25–54. <https://doi.org/10.1016/j.buildenv.2005.07.030>
- Yang, W., Wang, Z., Cui, J., Zhu, Z., & Zhao, X. (2015). 'Comparative study of the thermal performance of the novel green (planting) roofs against other existing roofs'. *Sustainable Cities and Society*, 16, 1–12. <https://doi.org/10.1016/j.scs.2015.01.002>
- Yang, J., Mohan Kumar, D. I., Pyrgou, A., Chong, A., Santamouris, M., Kolokotsa, D., et al. (2018). Green and cool roofs' urban heat island mitigation potential in tropical climate. *Solar Energy*, 173, 597–609. <https://doi.org/10.1016/j.solener.2018.08.006>
- Yang, X., Yao, L., Jin, T., Peng, L. L. H., Jiang, Z., Hu, Z., et al. (2018). 'Assessing the thermal behavior of different local climate zones in the Nanjing metropolis, China'. *Building and Environment*, 137, 171–184. <https://doi.org/10.1016/j.buildenv.2018.04.009>
- Yin, H., Kong, F., Dronova, I., Middel, A., & James, P. (2019). 'Investigation of extensive green roof outdoor spatio-temporal thermal performance during summer in a subtropical monsoon climate'. *The Science of the Total Environment*, 696, Article 133976. <https://doi.org/10.1016/j.scitotenv.2019.133976>
- Zhang, G., He, B.-J., & Dewancker, B. J. (2020). 'The maintenance of prefabricated green roofs for preserving cooling performance: A field measurement in the subtropical city of Hangzhou, China'. *Sustainable Cities and Society*, 61. <https://doi.org/10.1016/j.scs.2020.102314>
- Zhang, L., Fukuda, H., & Liu, Z. (2019). Households' willingness to pay for green roof for mitigating heat island effects in Beijing (China). *Building and Environment*, 150, 13–20. <https://doi.org/10.1016/j.buildenv.2018.12.048>